

Correcting Sampling Oscilloscope Timebase Errors With a Passively Mode-Locked Laser Phase Locked to a Microwave Oscillator

Jeffrey A. Jargon, *Senior Member, IEEE*, Paul D. Hale, *Senior Member, IEEE*, and C. M. Wang

Abstract—In this paper, we describe an apparatus for correcting the timebase errors when calibrating the response of an equivalent-time sampling oscilloscope using a passively mode-locked erbium-doped fiber laser that is phase locked to a microwave signal generator. This enables us to simultaneously correct both the random jitter and the systematic timebase distortion in the oscilloscope. As a demonstration of the technique, we measure the electrical pulse generated by a fast photodiode that is excited by our laser. We show that the pulse that is reconstructed using our technique has significantly lower uncertainty than the pulse that is reconstructed using a separate correction for timebase distortion followed by jitter deconvolution.

Index Terms—Mode-locked laser, phase-locked loop (PLL), sampling oscilloscope, timebase correction.

I. INTRODUCTION

A passively mode-locked laser emits a periodic train of ultrashort pulses by means of a saturable absorber to obtain self-amplitude modulation of the light inside the laser cavity [1]. This train of pulses in the time domain is equivalent to a frequency comb in the frequency domain, whose “comb teeth” are separated by integer multiples of the mode number. Such mode-locked lasers have applications in frequency metrology [2], electrooptic sampling [3], and optical fiber communication research [4]. Here, we describe the use of a passively mode-locked erbium-doped fiber laser (EDFL) as a stimulus source for exciting a high-speed photodiode. The photodiode, in turn, generates a short electrical pulse that is measured on the electrical channel of an equivalent-time sampling oscilloscope. If the photodiode is calibrated, as with an electrooptic sampling system in [5], this measurement can be used with the techniques in [6] to calibrate the complex frequency response of a high-speed sampling oscilloscope. Because EDFLs operate in the 1550-nm wavelength region used for long-haul

communications, they are well-suited for characterizing the response of optical oscilloscope channels, which are sometimes called reference receivers and can be used for measuring optical eye patterns. EDFLs produce pulses with durations on the order of 0.1–0.5 ps, which is typically more than an order of magnitude faster than the receiver that is being characterized, making possible high-accuracy measurements of the receiver response.

Sampling oscilloscopes typically have errors in the time at which the samples are taken, which can significantly affect the measurement and determination of the oscilloscope’s response. These errors can be decomposed into a random component, which is called jitter, and a systematic component, which is known as timebase distortion (TBD). Phase locking the repetition rate of the laser to a microwave signal generator enables us to employ the National Institute of Standards and Technology (NIST) timebase correction (TBC) method in [7] to correct for imperfections in the high-speed sampling oscilloscope’s timebase by simultaneously measuring two quadrature reference sinusoids and the calibration impulse. The two sinusoids, which originate from the microwave signal generator, allow the actual times at which the samples are taken by the oscilloscope to be accurately reconstructed with a covariance-based uncertainty analysis [8]. This method replaces the separate procedures described in [6] for estimating TBD [9] and jitter [10] and then jitter deconvolution [11] but does not replace the intermediate interpolation required before the Fourier transformation usually employed for deconvolution.

In this paper, we report a novel application of laser and phase-locked-loop (PLL) technology to the characterization of the timebase and acquisition channel of a sampling oscilloscope. Our apparatus and procedure have the advantages of TBC described in [7], allowing us to make more repeatable calibrations of the oscilloscope. In particular, after applying the NIST TBC algorithm, the residual jitter is reduced to approximately 200 fs, and the deconvolution of its effects requires little or no regularization. Furthermore, since the measurements required for correcting the timebase are simultaneously made with the oscilloscope calibration impulse, we need not worry about systematic differences in the TBD between when the impulse is measured and when the reference sinusoids are measured. For example, the TBD may change due to temperature changes or changes in the sampling rate, as described in [12, Ch. 4]. The mode-locked laser that is phase locked to an oscillator can also be used with commercially available TBC

Manuscript received December 17, 2008; revised July 14, 2009. First published October 9, 2009; current version published March 20, 2010. The Associate Editor coordinating the review process for this paper was Dr. Yves Rolain.

The authors are with the National Institute of Standards and Technology, Boulder, CO 80305 USA (e-mail: jargon@boulder.nist.gov).

Color versions of one or more of the figures in this paper are available online at <http://ieeexplore.ieee.org>.

Digital Object Identifier 10.1109/TIM.2009.2030929

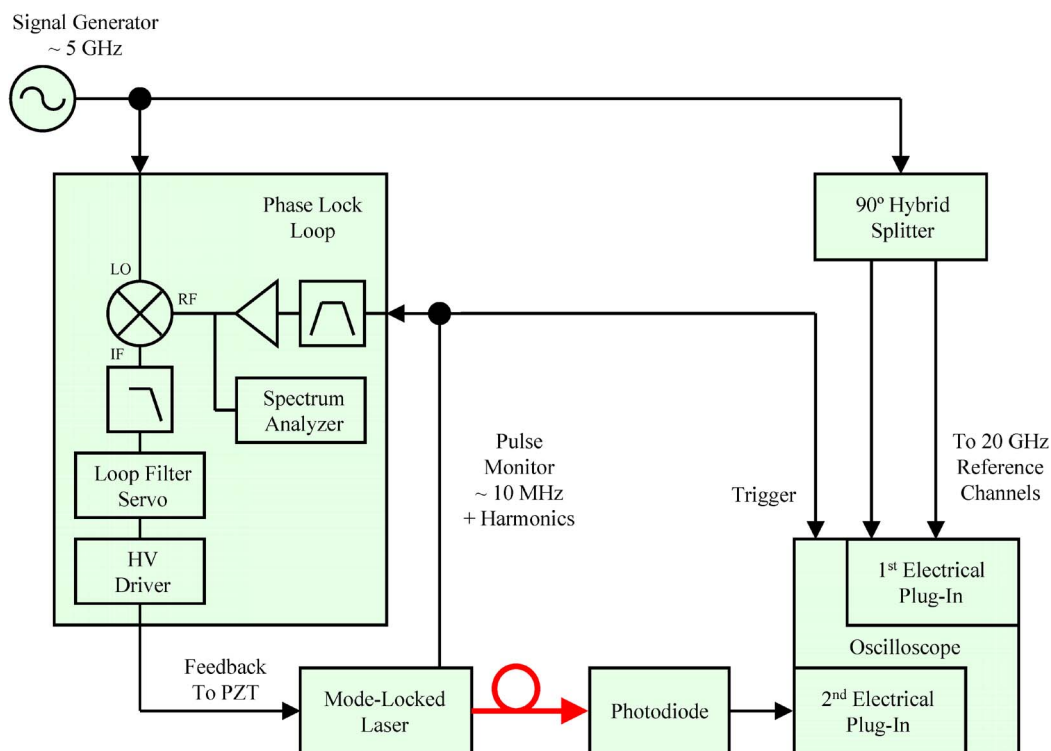


Fig. 1. Setup for measuring the response of timebase-corrected sampling oscilloscopes using a phase-locked passively mode-locked laser whose repetition rate is approximately 10 MHz.

equipment.^{1,2} However, the NIST TBC software package is freely available on the web [13], the techniques used are openly documented in [7], and the software gives access to the various elements used in determining the corrected timebase so that a statistical analysis can be made, as described in [8].

In the following sections, we describe the system configuration in detail and provide example measurements with comparisons between timebase error correction methods. To the best of our knowledge, this is the first report in the open literature of a mode-locked laser used with TBC algorithms for improved oscilloscope calibration.

II. PLL

Fig. 1 shows the configuration for measuring the response of timebase-corrected sampling oscilloscopes using a passively mode-locked EDFL that is phase locked to a microwave signal generator. The phase-locking circuit is similar to several others that have been used for controlling mode-locked lasers [14]–[16]. A low-phase-noise microwave signal generator operating at approximately 5 GHz has its output signal split so that half of it acts as a reference for the PLL and the other half is fed into the 90° hybrid splitter. The PLL locks the mode-locked laser's repetition frequency to the signal generator by adjusting the voltage on a piezoelectric transducer (PZT) that

¹Agilent 86107A precision timebase reference module. NIST does not endorse or guarantee this product. Other products may perform as well as or better than those listed here.

²Tektronix 82A04 phase reference module. NIST does not endorse or guarantee this product. Other products may perform as well as or better than those listed here.

controls the length of the laser cavity. Our technique requires that the oscilloscope have at least three channels. The oscilloscope is triggered by the electrical pulse train from the laser's pulse-monitor output and measures two quadrature reference sinusoids on the oscilloscope's first electrical plug-in. These sinusoids are used to correct imperfections in the oscilloscope's timebase. The laser provides short optical pulses to the photodiode connected to the oscilloscope's (third) electrical channel that is being calibrated.

The mode-locked EDFL produces a collimated optical beam with impulsive pulses that have a duration (full-width at half-maximum) of approximately 100 fs at a center wavelength of 1550 nm and a repetition rate of approximately 10 MHz. The laser has an electrical pulse-monitor output and an electrical input to a PZT for cavity-length control. The electrical pulse-monitor signal, which contains an electrical comb of frequencies at intervals of about 10 MHz, is fed into the PLL, which locks onto the 500th harmonic (about 5 GHz). The repetition rate of the laser can be tuned over a 600-Hz range by applying an external voltage from 0 to 1000 V to the PZT controller.

The PLL has two inputs, i.e., a reference signal from the signal generator and a signal from the laser's pulse monitor, and one output, i.e., a voltage for controlling the laser's PZT controller. The electrical pulse monitor signal is filtered with a 5-GHz bandpass filter and then amplified using a low-noise amplifier before being fed into the RF port of a double-balanced mixer. The input from the reference oscillator is fed into the local-oscillator (LO) port of the mixer. The resulting signal emerging from the intermediate-frequency (IF) port of the mixer contains a phase-error signal of the two inputs. A low-pass filter eliminates unwanted higher frequency products, and

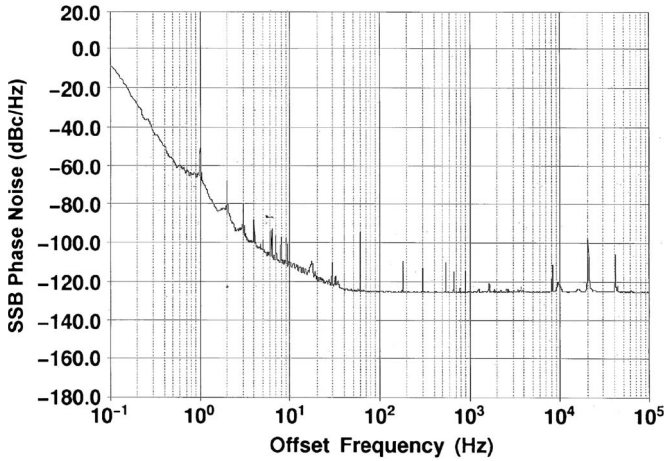


Fig. 2. Residual single-sideband phase noise of the laser's pulse-monitor signal as a function of the offset frequency from the laser repetition frequency of 10 MHz without a phase lock.

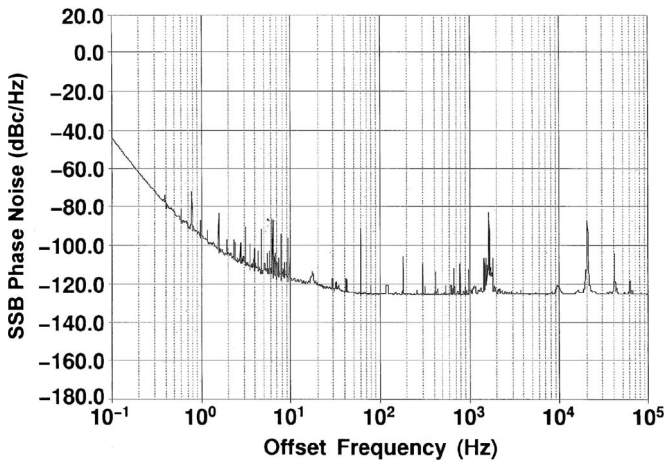


Fig. 3. Residual single-sideband phase noise of the laser's pulse-monitor signal as a function of the offset frequency from the laser repetition frequency of 10 MHz when phase locked to the microwave signal generator.

the resulting signal is fed into an NIST-designed loop filter and then into a high-voltage driver. This PLL continuously adjusts the voltage on the laser's PZT to maintain quadrature between the signals of the mode-locked laser and the reference signal, thus locking the laser repetition frequency to the signal generator, which also generates the two quadrature reference sinusoids for the TBC.

Phase-noise measurements were made on the 10-MHz pulse-monitor signal with and without a phase lock using a digital phase-noise measurement system [17]. This was done simply by splitting off a portion of the pulse-monitor signal, filtering it with a bandpass filter centered at 10 MHz, amplifying it with a low-noise amplifier, and feeding the resulting signal into the digital phase-noise measurement system, along with a 10-MHz reference signal from a very low phase-noise quartz oscillator. Fig. 2 shows the residual single-sideband phase noise (in decibels relative to the carrier per hertz) of the laser's pulse-monitor signal as a function of the offset frequency from the laser repetition frequency of 10 MHz without a phase lock. Fig. 3 shows the same measurement with a phase lock. From the two graphs, it can be seen that locking the laser to the

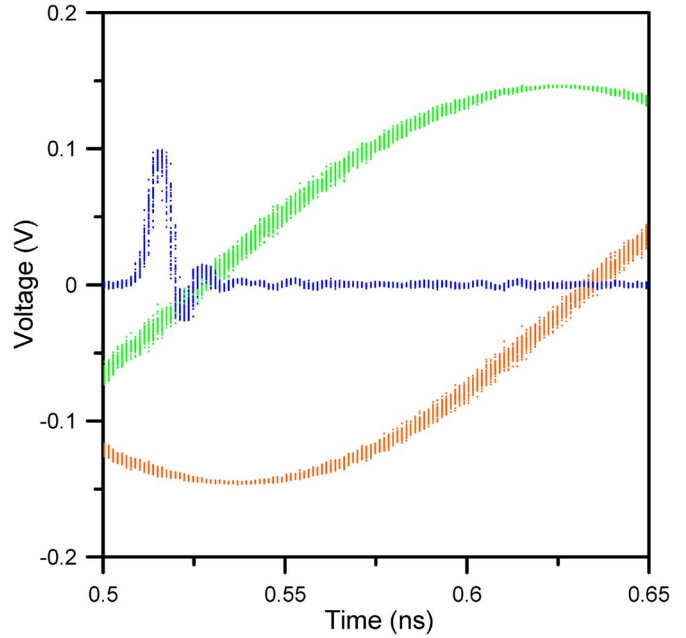


Fig. 4. Oscilloscope measurements of an optical pulse simultaneously measured with two 5.000844-GHz reference sinusoids. Notice that the noise at the sinusoid maxima is much less than the noise where the sinusoids are rapidly changing, indicating that the noise is dominated by jitter.

microwave signal generator significantly reduces the phase noise at offset frequencies below 20 Hz, which is consistent with the bandwidth setting of the NIST-designed loop filter at 15.9 Hz.

III. MEASUREMENTS

In this section, we show how the configuration described earlier can be used to correct for timebase errors when the impulse generated by a fast photodiode is measured by simultaneously measuring two reference sinusoids. To realize this simultaneity, the oscilloscope must have an architecture that activates the samplers in the channels from a single trigger event and allows the transfer of the synchronously sampled data to an external computer for postprocessing. As explained in [7], this method generates a new timebase by assuming that the jitter on all of the oscilloscope channels is sufficiently correlated, such that an estimate of the timebase error based on a measurement of the sinusoids in channels 1 and 2 can be used to correct the timebase errors when measuring the signal of interest in channel 3. The conventional timebase of the oscilloscope is considered an initial estimate of the time at which samples are taken and is used to characterize the distortion in the two reference sinusoids. We estimate the new timebase from the sinusoids using the weighted “error-in-variables” approach in [18] that accounts for the relative contributions of additive noise and timing error.

Fig. 4 shows an actual measurement of an optical pulse simultaneously measured with two reference sinusoids. The frequency of the sinusoids was 5.000866 GHz, which is the 500th harmonic of the 10.0017-MHz repetition rate of the laser. The optical pulse was measured with a photodiode that has an approximately 90-GHz (optical) bandwidth, and was connected to the oscilloscope's electrical channel that has an

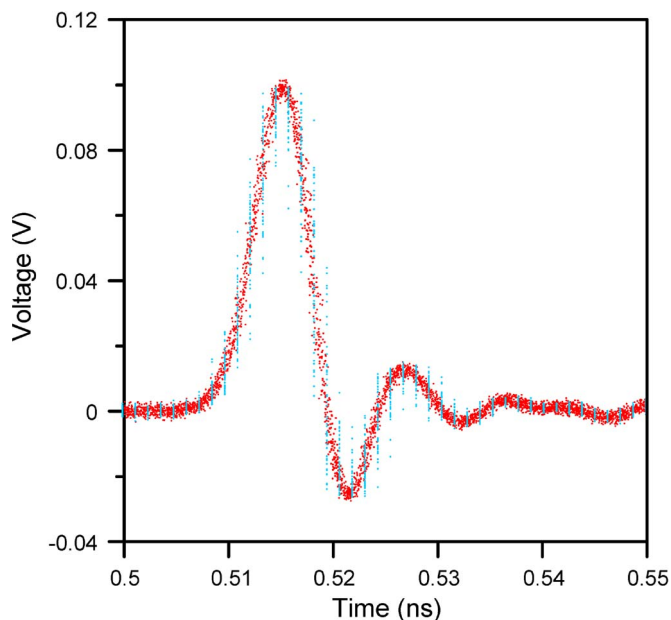


Fig. 5. One hundred waveforms of the as-measured (evenly spaced in time) and timebase-corrected pulses (distributed in time). The measured pulses have an initial RMS jitter of 0.81 ps, while the timebase-corrected pulses have a residual RMS jitter of 0.22 ps.

approximately 90-GHz bandwidth. The RMS additive noise in this channel was 0.9 mV. The electrical channels used to measure the sinusoids have a full bandwidth of 20 GHz but were set (through the oscilloscope user interface) to have a bandwidth of 12.4 GHz to reduce the RMS additive noise in the sinusoid measurements to 0.2 mV. All three signals were measured using 8192 points over a 5.1-ns epoch. We also made two additional (nonsynchronous) measurements of quadrature sinusoids at 4.92085 (the 492nd harmonic of the repetition rate) and 5.32092 GHz (the 532nd harmonic). We made use of the additional sinusoids to provide information on the harmonic distortion of the measurement channel, as described in [7] and [19]. To provide the statistics of our measurements, we acquired 1000 waveforms and partitioned the measurements into ten sets of 100 measurements. We used the NIST TBC software [13] to correct the timebase errors in all the measurements with a weighting factor of $4.7 \text{ ns}^2/\text{V}^2$.

IV. RESULTS AND COMPARISON

In this section, we evaluate the results of our apparatus and TBC procedure by estimating the jitter before and after correction and characterize the variation of ten separate estimates of the jitter and the pulsewidth. As a benchmark, we also compare these results with the variation observed when using the method in [6], where TBD and jitter are separately corrected. Here, we refer to this method as the “old method.”

A. As-Measured Results

Fig. 5 plots a set of 100 waveforms as measured. Note that the as-measured data fall at equally spaced times, as mandated by the standard assumptions of normal oscilloscope operation. We calculated the pointwise mean and standard deviation of each of

the ten sets of 100 as-measured waveforms. We estimated the jitter variance of the ten as-measured sets of waveforms using the first-order Taylor series expansion

$$s_{\text{Total}}^2 \approx s_{\text{N}}^2 + \hat{\sigma}_{\text{J}}^2 \left(\frac{dy}{dt} \right)^2 \quad (1)$$

where s_{Total} is the signal standard deviation at a given time, s_{N} is the additive noise standard deviation, $\hat{\sigma}_{\text{J}}^2$ is the estimated jitter variance, and dy/dt is the derivative of the true time-domain waveform. In this case, we must approximate the derivative using the measured average and a finite-difference technique. Furthermore, we did not attempt correction for the bias in the estimated jitter, which is typically about 10% of the actual jitter. Finally, we estimated the half-maximum pulse duration of each of the ten averaged pulse waveforms using linear interpolation to estimate the 50% crossing level. The mean and standard deviation of these ten estimates are shown in Table I along with the mean of the ten jitter estimates.

B. Results of TBC (New Method)

We first used the NIST TBC software [13] to correct for random and systematic timebase errors. The results of this correction are shown in Fig. 5. To characterize the residual jitter in these corrected waveforms, we used a procedure similar to that described earlier. However, to calculate a pointwise estimate of the standard deviation for each measurement set for use in (1), we needed to interpolate the data to 4096 points spaced uniformly over a 5-ns epoch. This task is complicated by the jitter, whose standard deviation is roughly 3/4 of the nominal interval between samples. While our initial waveform was sampled densely enough to linearly interpolate with adequate accuracy, this is not necessarily the case for a single timebase-corrected waveform. Because the jitter is relatively large, the interval between samples after correction can be significantly larger than the nominal sampling interval (before correction). Linear and higher order interpolation of this undersampled waveform can cause significant errors.

To increase the density of samples for interpolation, we merged two consecutively measured waveforms from a given data set and then used linear interpolation³ to reconstruct the waveform on the desired uniformly spaced time grid. We repeated this procedure 50 times for each consecutive pair in each of the ten measurement sets. Visual inspection shows that the voltage spread of the interpolated data at each time matched the spread of the uninterpolated data cloud in Fig. 5. From the 50 reconstructed waveforms, we calculated the mean waveform, and the standard deviation at each time to use (1) to estimate the variance $\hat{\sigma}_{\text{J-TBC}}^2$ of the jitter remaining after TBC. The mean of the ten jitter estimates is reported in Table I.

Using our estimate of the jitter for each data set, we corrected the mean waveform for the effects of the residual jitter using deconvolution, where the residual jitter represents the incoherence between the measurements of the sine waves and the

³We use linear interpolation for convenience and consistency here, and we do not claim that linear interpolation is in some way optimal. For a comparison of various interpolation schemes, see [20] and [21] and the references therein.

TABLE I
JITTER AND FULL-WIDTH AT HALF-MAXIMUM OF MEASURED PULSE WAVEFORMS AS MEASURED AND WITH THE OLD AND NEW METHODS FOR CORRECTING TIMEBASE ERRORS

	As-measured	TBC method (new)	Separate correction for TBD + jitter (old)
Mean pulse duration (ten estimates), ps	6.14	5.87	5.78
Standard deviation of pulse duration, ps	0.14	0.03	0.20
Typical jitter (mean of ten estimates), ps	0.81	0.22	—

measurements of the pulse. Each mean waveform was Fourier transformed to the frequency domain to obtain $\bar{Y}(\omega)$ and corrected for residual jitter using the estimated jitter variance from the waveform obtained from the TBC procedure

$$\bar{Y}_C = \exp\left(\frac{1}{2}\hat{\sigma}_{J-TBC}^2\omega^2\right)\bar{Y}. \quad (2)$$

The corrected time-domain waveform \bar{y}_C was obtained as the inverse Fourier transform of \bar{Y}_C . This procedure was repeated for each of the ten different sets of corrected waveforms. We estimated the half-maximum pulse duration of the ten averaged pulse waveforms using linear interpolation. The mean and standard deviation of these ten estimates are shown in Table I.

C. Results of Separate Correction for TBD and Jitter (Old Method)

For comparison, we also corrected the as-measured data with a simplified version of the method described in [6], which separately corrects for TBD and jitter. We estimated the TBD from the first set of 100 measurements using the method in [9]. This TBD was used to correct all ten sets of 100 waveforms. Linear interpolation was used to reconstruct the waveform on the desired uniformly spaced time grid. In this case, the TBD is a slowly varying function, and the linear interpolation of a single waveform gives an acceptable approximation. After correction for TBD and interpolation, we estimated the jitter variance $\hat{\sigma}_{TBD-J}^2$ of each data set. We then calculated the mean waveform \bar{y}_{TBD} for each set of measurements. Each mean waveform was Fourier transformed to the frequency domain to obtain $\bar{Y}_{TBD}(\omega)$ and corrected for jitter using the estimated jitter variance $\hat{\sigma}_{TBD-J}^2$ from the interpolated waveform

$$\bar{Y}_{TBD-J} = \exp\left(\frac{1}{2}\hat{\sigma}_{TBD-J}^2\omega^2\right)\bar{Y}_{TBD}. \quad (3)$$

The corrected time-domain waveform \bar{y}_{TBD-J} was obtained as the inverse Fourier transform of \bar{Y}_{TBD-J} . We did not attempt any form of regularization of the deconvolution of (3), and we comment more on this choice in the next section. We repeated this procedure for each of the ten sets of 100 waveforms, which had already been corrected for TBD. We estimated the half-maximum pulse duration of the ten averaged pulse waveforms using linear interpolation. The mean and standard deviation

of these ten estimates are also shown in Table I. We did not estimate the remaining jitter after correction.⁴

D. Comparison

We used statistical hypothesis testing to determine if the estimated pulse durations are significantly different and if the standard deviations of the estimates are significantly different. The 95% confidence intervals for pulse duration calculated from the three means and standard deviations listed in Table I (with 10 DOF) are (5.828, 6.452), (5.803, 5.937), and (5.334, 6.226). Since these intervals overlap, we conclude that the pulse durations are not significantly different from each other. This is because the jitter in the original as-measured data is small compared to the pulse duration and because the standard deviation in the durations estimated from the as-measured data and the duration estimated from separate correction are both fairly large.

The test statistic for the equality of the pulsewidth standard deviation is the variance ratio $F = 0.2^2/0.03^2 = 44.4$. The p -value of the test is the probability of observing a realization of a random variable with an F distribution with 10 DOF in the numerator and 10 DOF in the denominator that is greater than or equal to 44.4. This probability is less than 0.00001. That is, the difference between the variations in estimated pulsewidth after reconstruction using the two different techniques is very significant.

Furthermore, the pulse as estimated with the TBC procedures has about four times less jitter than the raw measurements. The old method for separately correcting TBD and jitter degraded the precision in determining the pulse duration by a factor of 6.7 compared to the TBC method and is degraded by a factor of 1.4 compared the as-measured data. This is because of noise amplification in the deconvolution of (3). Fig. 6 shows $20 \log(|\bar{Y}_{TBD}|/|\bar{Y}_C|)$ for one set of 100 measurements along with the expected roll-off $20 \log(\exp(-1/2\hat{\sigma}_J^2\omega^2))$ due to jitter. We see that the waveform spectrum magnitude $|\bar{Y}_{TBD}|$ does indeed decrease with frequency, relative to the waveform spectrum magnitude $|\bar{Y}_C|$, as expected. Fig. 7 shows $20 \log(|\bar{Y}_{TBD-J}|/|\bar{Y}_C|)$, which is more flat, indicating that the effects of jitter have been removed and that the TBC procedure

⁴Although the jitter deconvolution could be applied to each timebase-corrected waveform (instead of the average) and (1) could be applied to estimate something similar to a “residual jitter,” it is not clear how this result should be interpreted, and the discussion of this interpretation lies outside the scope of this paper, so we leave the jitter entry for this technique blank.

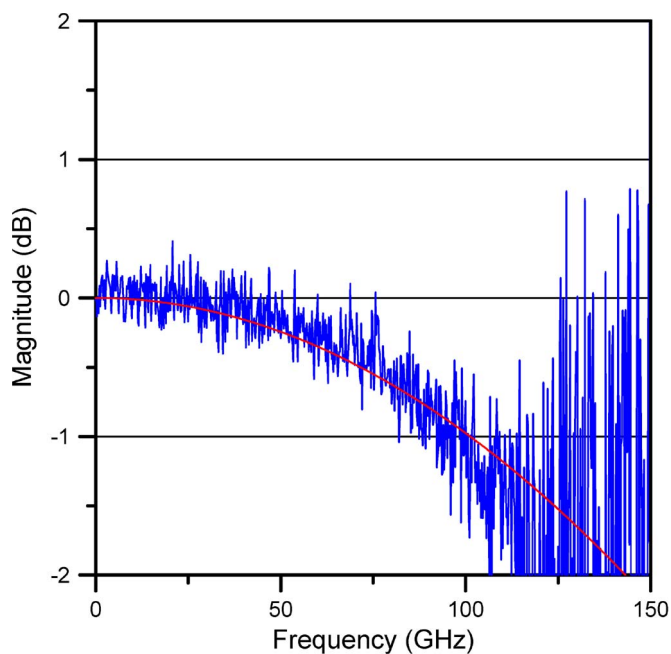


Fig. 6. Jagged trace of $20 \log(|\bar{Y}_{TBD}|/|\bar{Y}_C|)$ rolls off along the smooth curve of $20 \log(\exp(-1/2\hat{\sigma}_j^2\omega^2))$, indicating the presence of jitter in the waveform that has been corrected only for TBD but not yet for the effects of jitter.

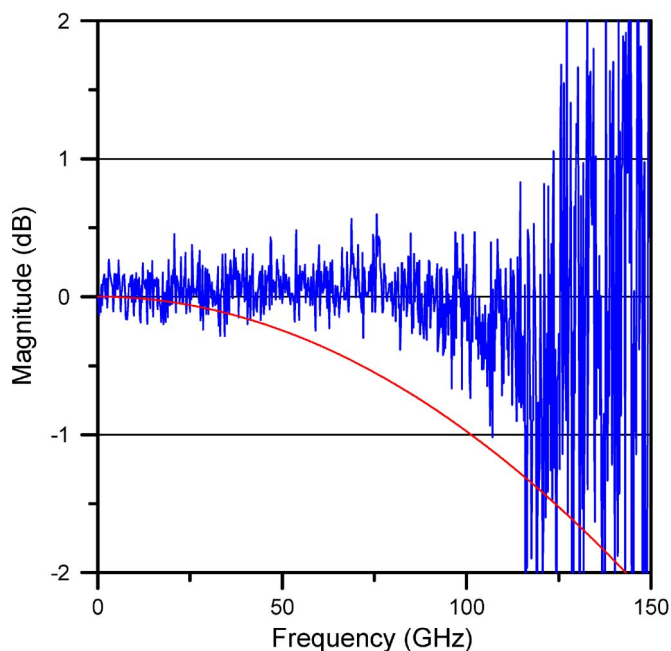


Fig. 7. Jagged trace of $20 \log(|\bar{Y}_{TBD-J}|/|\bar{Y}_C|)$ is flat, up to about 80 GHz, indicating that the two TBC methods, which are totally independent of each other, estimate essentially the same response function, within the noise variation in the system.

and the old procedure for separately removing the effects of TBD and jitter give, on the average, similar results up to about 100 GHz.

Finally, Fig. 8 shows the magnitude spectra of averaged waveforms reconstructed using both approaches. The noise of the waveform reconstructed using the old method clearly increases above 150 GHz because of the amplifying nature of the deconvolution in (3). Presumably, this is the cause of

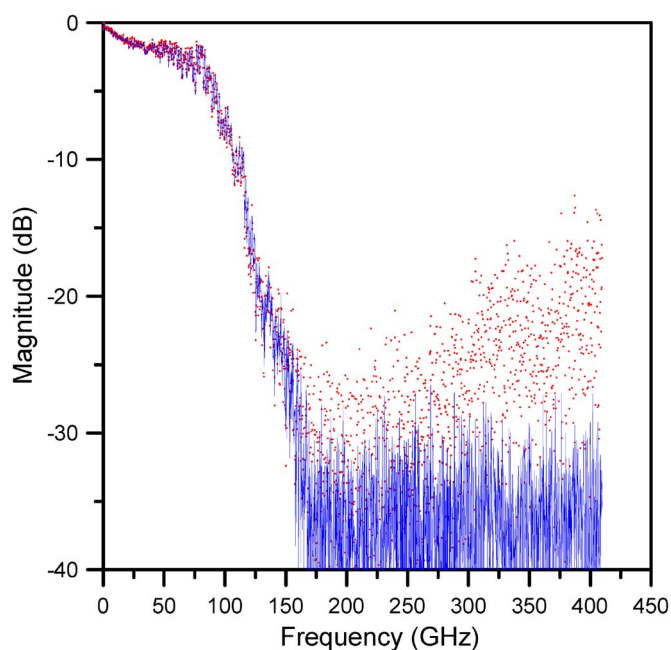


Fig. 8. Trace: $20 \log |\bar{Y}_C/\bar{Y}_C(0)|$. Dots: $20 \log |\bar{Y}_{TBD-J}/\bar{Y}_{TBD-J}(0)|$. Note that, in the latter case, the noise above about 150 GHz has been amplified by the deconvolution process.

the decreased precision in determining the pulse duration. For the purposes of this paper, we chose to not regularize the deconvolution so that the associated noise could be highlighted. We note that if the pulse were reconstructed on a time grid with 8192 points, the frequency spectrum would be extended to beyond 800 GHz, and the noise would be amplified to such an extent as to render the time-domain representation of the waveform useless. Clearly, a regularization strategy could be employed to reduce the noise, in the case of 4096-point reconstruction, and regularization would be required in the case of the 8192-point reconstruction, at the expense of adding systematic error in both cases.

V. DISCUSSION

We have described an apparatus and procedures for making timebase-corrected measurements of electrical or optical pulses that are generated with a passively mode-locked laser that is phase locked to a microwave signal generator. With the laser phase locked to the quadrature reference sinusoids, it is now possible to simultaneously correct for random jitter and systematic TBD in the oscilloscope when measuring a laser pulse. The resulting waveform is randomly sampled. We have not explored the ramifications here, but if the jitter standard deviation is comparable to the sample spacing, a superposition of these randomly sampled waveforms can actually have a mean sample spacing substantially less than the target sample spacing of the as-measured waveform, effectively increasing the Nyquist frequency of the measurement.

The apparatus and TBC procedures we have described here can also be used to calibrate a sampling oscilloscope that has an optical input and is sometimes referred to as a reference receiver. Such receivers are often used to characterize signals used in digital optical communications, particularly through

the use of eye pattern measurements [22]. As mentioned in Section I, mode-locked EDFLs are well suited for characterizing the response of reference receivers because they operate in the 1550-nm wavelength region in which the receivers for long-haul communications are used. EDFLs produce pulses with durations on the order of 0.1–0.5 ps, which is typically more than an order of magnitude faster than the receiver being characterized, making possible high-accuracy measurements of the receiver response.

ACKNOWLEDGMENT

The authors would like to thank N. Newbury and J. Schlager for their helpful discussions regarding phase-locked loops, A. Dienstfrey for the helpful discussions regarding interpolation, and T. Dennis for his helpful comments regarding the preparation of this manuscript. This work is a contribution of the U.S. government, and is not subject to copyright.

REFERENCES

- [1] U. Keller, "Recent developments in compact ultrafast lasers," *Nature*, vol. 424, no. 6950, pp. 831–838, Aug. 2003.
- [2] N. R. Newbury and W. C. Swann, "Low-noise fiber-laser frequency combs," *J. Opt. Soc. Amer. B, Opt. Phys.*, vol. 24, no. 8, pp. 1756–1770, Aug. 2007.
- [3] D. F. Williams, P. D. Hale, T. S. Clement, and J. M. Morgan, "Calibrating electro-optic sampling systems," in *Proc. IEEE MTT-S Int. Microw. Symp. Dig.*, May 2001, vol. 3, pp. 1527–1530.
- [4] "Testing with femtosecond pulses," Calmar Optcom White Paper, Sep. 2003. Rev.1.1.
- [5] D. F. Williams, A. Lewandowski, T. S. Clement, C. M. Wang, P. D. Hale, J. M. Morgan, D. A. Keenan, and A. Dienstfrey, "Covariance-based uncertainty analysis of the NIST electrooptic sampling system," *IEEE Trans. Microw. Theory Tech.*, vol. 54, no. 1, pp. 481–491, Jan. 2006.
- [6] T. S. Clement, P. D. Hale, D. F. Williams, C. M. Wang, A. Dienstfrey, and D. A. Keenan, "Calibration of sampling oscilloscopes with high-speed photodiodes," *IEEE Trans. Microw. Theory Tech.*, vol. 54, no. 8, pp. 3173–3181, Aug. 2006.
- [7] P. D. Hale, C. M. Wang, D. F. Williams, K. A. Remley, and J. D. Wepman, "Compensation of random and systematic timing errors in sampling oscilloscopes," *IEEE Trans. Instrum. Meas.*, vol. 55, no. 6, pp. 2146–2154, Dec. 2006.
- [8] C. M. Wang, P. D. Hale, and D. F. Williams, "Uncertainty of timebase corrections," *IEEE Trans. Instrum. Meas.*, vol. 58, no. 10, pp. 3468–3472, Oct. 2009.
- [9] C. M. Wang, P. D. Hale, and K. J. Coakley, "Least-squares estimation of time-base distortion of sampling oscilloscopes," *IEEE Trans. Instrum. Meas.*, vol. 48, no. 6, pp. 1324–1332, Dec. 1999.
- [10] K. J. Coakley, C. Wang, P. D. Hale, and T. S. Clement, "Adaptive characterization of jitter noise in sampled high-speed signals," *IEEE Trans. Instrum. Meas.*, vol. 52, no. 5, pp. 1537–1547, Oct. 2003.
- [11] W. L. Gans, "The measurement and deconvolution of time jitter in equivalent-time waveform samples," *IEEE Trans. Instrum. Meas.*, vol. IM-32, no. 1, pp. 126–133, Mar. 1983.
- [12] F. Verbeyst, "Contributions to large-signal analysis," Ph.D. dissertation, Vrije Universiteit Brussel, Brussels, Belgium, Sep. 2006.
- [13] P. D. Hale, C. M. Wang, D. F. Williams, K. A. Remley, and J. Wepman, Time Base Correction (TBC) Software Package 2005. [Online]. Available: http://www.boulder.nist.gov/div815/HSM_Project/Software.htm
- [14] M. J. W. Rodwell, D. M. Bloom, and K. J. Weingarten, "Subpicosecond laser timing stabilization," *IEEE J. Quantum Electron.*, vol. 25, no. 4, pp. 817–827, Apr. 1989.
- [15] D. R. Walker, D. W. Crust, W. E. Sleat, and W. Sibbett, "Reduction of phase noise in passively mode-locked lasers," *IEEE J. Quantum Electron.*, vol. 28, no. 1, pp. 289–296, Jan. 1992.
- [16] J. B. Schlager, B. E. Callicot, R. P. Mirin, and N. A. Sanford, "Passively mode-locked waveguide laser with low residual jitter," *IEEE Photon. Technol. Lett.*, vol. 14, no. 9, pp. 1351–1353, Sep. 2002.
- [17] J. Grove, J. Hein, J. Retta, P. Schweiger, W. Solbrig, and S. R. Stein, "Direct-digital phase-noise measurement," in *Proc. IEEE 50th Anniversary Joint Conference Int. Ultrason., Ferroelectr., Freq. Control*, Aug. 2004, pp. 287–291.
- [18] ODRPACK, [Online]. Available: <http://www.netlib.org/netlib/odrpac/>
- [19] H. C. Reader, D. F. Williams, P. D. Hale, and T. S. Clement, "Comb-generator characterization," *IEEE Trans. Microw. Theory Tech.*, vol. 56, no. 2, pp. 515–521, Feb. 2008.
- [20] Y. Rolain, J. Schoukens, and G. Vandersteen, "Signal reconstruction for non-equidistant finite length sample sets: A 'KIS' approach," *IEEE Trans. Instrum. Meas.*, vol. 47, no. 5, pp. 1046–1052, Oct. 1998.
- [21] M. Unser, "Sampling-50 years after Shannon," *Proc. IEEE*, vol. 88, no. 4, pp. 569–587, Apr. 2000.
- [22] D. Derickson, Ed., *Fiber Optic Test and Measurement*. Englewood Cliffs, NJ: Prentice-Hall, 1998.



Jeffrey A. Jargon (M'98–SM'01) received the B.S., M.S., and Ph.D. degrees in electrical engineering from the University of Colorado at Boulder, Boulder, in 1990, 1996, and 2003, respectively.

Since 1990, he has been a Staff Member with the National Institute of Standards and Technology, Boulder, CO, where he has conducted research in the areas of vector network analyzer calibrations and microwave metrology and is currently a member of the High-Speed Measurements Project, Optoelectronics Division. He is the author of more than 60 published

technical articles.

Dr. Jargon is a Registered Professional Engineer in the State of Colorado. He is a member of Tau Beta Pi and Eta Kappa Nu. He is the recipient of four best paper awards, an URSI Young Scientist Award, and a Department of Commerce Silver Medal award.



Paul D. Hale (SM'01) received the Ph.D. degree in applied physics from the Colorado School of Mines, Golden, in 1989.

Since 1989, he has been with the Optoelectronics Division, National Institute of Standards and Technology (NIST), Boulder, CO, where he conducts research on broadband optoelectronic device and signal metrology and has been the Leader of the High-Speed Measurements Project, Sources and Detectors Group, since 1996. He is the author of more than 60 technical publications. His current technical

work focuses on extending both time- and frequency-domain optoelectronic measurements to beyond 110 GHz, implementing a novel covariance-based uncertainty analysis that can be used for both time- and frequency-domain quantities, and disseminating NIST traceability through high-speed electronic and optoelectronic measurement services.

Dr. Hale was an Associate Editor of *Optoelectronics/Integrated optics* for the *IEEE JOURNAL OF LIGHTWAVE TECHNOLOGY* from June 2001 to March 2007. He is the recipient of the Department of Commerce Bronze, Silver, and Gold Medal awards, two ARFTG Best Paper Awards, and the NIST Electrical Engineering Laboratory's Outstanding Paper Award.



C. M. "Jack" Wang received the Ph.D. degree in statistics from Colorado State University, Fort Collins, in 1978.

Since 1988, he has been with the Statistical Engineering Division, National Institute of Standards and Technology, Boulder, CO. He is the author of more than 70 journal articles. His research interests include statistical metrology and the application of statistical methods to physical sciences.

Dr. Wang is a Fellow of the American Statistical Association (ASA). He is the recipient of the Department of Commerce Bronze Medal awards and several awards from ASA.